


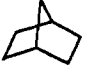


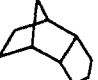
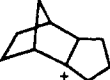


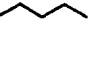
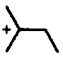


Figure 1. The reaction of norbornane with CCl_3^+ in the $\text{SbF}_5/\text{CCl}_4$ matrix: (a) starting material; (b–d) after successive warming from 77 to 150 K (the signals of 2-norbornyl cation are labeled with arrows).

Table II. Experimental Infrared Frequencies of Carbocations Generated in the Matrix Experiment at 150 K

precursor	ion	freq, cm^{-1}
		2910 s, 2850 s, 2750 s, 1456 m, 1400 m, 1310 vs, 1270 vs, 1210 m, 1150 w, 1105 w, 980 m, 910 m, 900 w
		3100 m, 2970 m, 2940 m, 1480 s, 1430 vs, 1380 s, 1350 vs, 1300 vs, 1280 s, 1245 w, 1235 vw, 1225 m, 1150 m, 1125 s, 1100 s, 1090 m, 1035 m, 980 m, 965 w, 920 w, 865 s
		2890 s, 2840 w, 1480 s, 1450 m, 1435 vw, 1350 m, 1320 m, 1255 m, 1190 w, 1170 s, 1150 w, 1115 vw, 1100 w, 1080 s, 1070 s, 1005 s, 973 s, 900 s
		2950 m, 1485 s, 1455 s, 1215 s, 1150 m, 1105 s, 980 s, 915 s
		2955 m, 2880 w, 2770 w, 1460 s, 1380 m, 1360 m, 1310 m, 1265 m, 1215 m, 1150 vs, 1100 s, 980 vs, 915 vs, 900 s
		2830 m, 1465 m, 1300 s, 1280 w, 1270 w, 1100 m, 1085 w, 1040 vs, 980 s, 910 w, 900 m

method is shown in Figure 1 for the reaction of norbornane with CCl_3^+ . The characteristic strong absorption band at 1040 cm^{-1} assigned to the C–Cl stretching vibration of CCl_3^+ gradually diminishes in intensity with the simultaneous appearance of bands characteristic for the 2-norbornyl cation.^{6b} Also, in the C–H stretching region two new weak bands ascribed to chloroform could be observed. In this manner carbocations listed in Table II have been prepared and characterized by (a) quenching with water to the corresponding alcohols and (b) their IR spectra, which were identical with the ones obtained⁶ from (cyclo)alkyl chlorides as precursors. The IR spectra of so-prepared carbocations were in most cases of a better quality than when alkyl chlorides were used as starting material.

In the experiment with *endo*-trimethylenenorbornane, the formation of a tertiary carbocation could be observed which was not the 1-adamantyl cation as the most stable of all $\text{C}_{10}\text{H}_{15}^+$ ions. Recently, Olah, Schleyer, and their collaborators^{10,11} have shown that the first intermediate generated from trimethylenenorbornane at $-60\text{ }^\circ\text{C}$ is the 5,6-trimethylene-4-norbornyl cation. Since in the Schleyer–Donaldson mechanism¹² of this rearrangement all intermediary ions are higher in energy, it is not surprising that also in the matrix the reaction is confined to the formation of the first unrearranged ion.

These experiments also shed some light on the mechanism of cationic rearrangements which were observed in the solid state below 150 K.¹³ Since reaction 2 can take place by only an *intermolecular* hydride abstraction, it is likely that in cases where *intramolecular* hydride shifts are precluded by symmetry or other reasons, these rearrangements follow the *intermolecular* path.

Acknowledgment. This work was supported by the Research Council of Croatia and the National Science Foundation (U.S.), Grant No. 841.

Supplementary Material Available: IR spectra of CCl_3^+ and starting CCl_4 , of CHCl_2^+ and starting CHCl_3 , and of $(\text{ClCH}_2)_2\text{Cl}^+$ and starting CH_2Cl_2 , all recorded between 77 and 150 K (3 pages). Ordering information is given on any current masthead page.

(10) Olah, G. A.; Farooq, O. *J. Org. Chem.* **1986**, *51*, 5410.

(11) Olah, G. A.; Prakash, G. K. S.; Shih, J. G.; Krishnamurthy, V. V.; Mateescu, G. D.; Liang, G.; Sipos, G.; Buss, V.; Gund, T. M.; Schleyer, P. v. R. *J. Am. Chem. Soc.* **1985**, *107*, 2764.

(12) Fort, R. C., Jr. *Adamantane, The Chemistry of Diamond Molecules*; Marcel Dekker: New York, 1976.

(13) Unpublished results from this laboratory; see also footnote 7 in ref 6b.

Novel Noninvasive in Situ Probe of Protein Structure and Dynamics

M. Négrerie,[†] S. M. Bellefeuille,[†] S. Whitham,[‡] J. W. Petrich,^{*†} and R. W. Thornburg^{*‡}

Department of Chemistry and
Department of Biochemistry and Biophysics
Iowa State University, Ames, Iowa 50011

Received May 21, 1990

7-Azatriptophan is an ideal noninvasive in situ probe of protein structure and dynamics and provides an alternative to the use of tryptophan. 7-Azatriptophan affords a single-exponential fluorescence decay in aqueous solution, unlike tryptophan. Its absorption and fluorescence spectra are distinguishable from those of tryptophan. Its fluorescence spectrum and lifetime are sensitive to the environment. It can be used in peptide synthesis, and it can be incorporated into bacterial protein. These facts render 7-azatriptophan a unique probe that has the potential for widespread use.

Tryptophan has been the most common optical probe of protein structure and dynamics.^{1,2} There are, however, two major problems attendant to its use in fluorescence measurements. First, since it is a naturally occurring amino acid, there are often several tryptophans whose emission must be distinguished in a protein molecule. Second, the fluorescence decay of tryptophan itself in aqueous solution is nonexponential.^{3–6} It is clearly desirable to

* To whom correspondence should be addressed.

[†] Department of Chemistry.

[‡] Department of Biochemistry and Biophysics.

(1) Beechem, J. M.; Brand, L. *Annu. Rev. Biochem.* **1985**, *54*, 43.

(2) Creed, D. *Photochem. Photobiol.* **1984**, *39*, 537.

(3) Szabo, A. G.; Rayner, D. M. *J. Am. Chem. Soc.* **1980**, *102*, 554.

(4) Petrich, J. W.; Chang, M. C.; McDonald, D. B.; Fleming, G. R. *J. Am. Chem. Soc.* **1983**, *105*, 3824.

Table I. Fluorescence Properties of 7-Azatriptophan and Its Derivatives

compound/solvent	absorptn max, ^a nm	emissn max, ^b nm	fluorescence lifetime: τ , ^b ps	detectn wavelength, nm
7-azatrp/H ₂ O, pH 7	288	410	780	$\lambda > 320$
7-azatrp/methanol	285	390	151	$320 < \lambda < 480$
7-azatrp/butanol	290	390	100	$\lambda > 350$
7-azaindole/H ₂ O, pH 7	289	398	915	$\lambda > 320$
7-azaindole/methanol	288	370	140	$320 < \lambda < 480$
7-azaindole/butanol	288	367	252	$320 < \lambda < 480$
7-azaindole/methylcyclohexane	280	329	1666	$320 < \lambda < 380$
<i>t</i> -BOC-7-azatrp ^c /H ₂ O, pH 7	292	416	635	$\lambda > 320$
<i>t</i> -BOC-7-azatrp ^c /methanol	292	400	133	$320 < \lambda < 480$
NAC-Pro-7-azatrp-Asn-NH ₂ ^c /H ₂ O, pH 7	290	414	870	$\lambda > 320$

^aTemperature = 28 °C. ^b $\lambda_{\text{ex}} = 285$ nm, 20 °C. For solvents other than water, a second band that is red-shifted appears in the fluorescence spectrum. This band has been attributed to a tautomeric form of 7-azaindole.¹³⁻¹⁷ Here, only emission from the principal (or blue-shifted) band is reported. The error in the measured lifetimes is less than 3%. ^cThe integrity of the derivatives was measured by chemical ionization and fast atom bombardment. Racemic mixtures resulting from the 7-azatriptophan starting material were separated by HPLC. The spectroscopy of the isolated D and L forms is identical under the conditions given in the table. The detailed photophysics and the synthesis and purification of the derivatives will be discussed in detail elsewhere.

use a probe whose fluorescence decay is single exponential in order to avoid difficulties in interpreting the fluorescence or anisotropy decays of the probe when it is incorporated in a peptide or a protein.⁷⁻¹²

The steady-state absorption and fluorescence properties of 7-azatriptophan are sufficiently different from those of tryptophan that selective excitation and detection may be effected (Figure 1 and Table I). The absorption maximum of 7-azatriptophan is red-shifted by 10 nm with respect to that of tryptophan. There is also a significant red shift of about 70 nm of the maximum of the fluorescence spectrum of 7-azatriptophan with respect to that of tryptophan. We have measured the fluorescence decay of an equimolar mixture of 7-azatriptophan and tryptophan as a function of excitation and detection wavelength (Figure 1). The data are remarkable for two reasons. First, as opposed to the fluorescence decay of aqueous tryptophan at pH 7, the fluorescence decay of 7-azatriptophan is single exponential. This result holds across the emission band and over the pH range we have studied, from 4 to 13. The monoexponential fluorescence decay in itself indicates the enormous advantage of using 7-azatriptophan instead of tryptophan as a fluorescent probe. Second, the equimolar

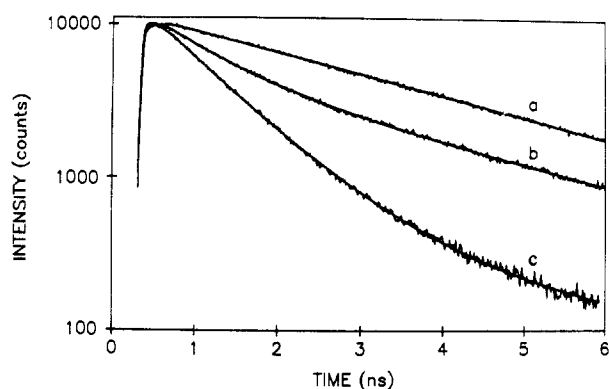


Figure 1. Fluorescence lifetime measurements at pH 7 and 20 °C. (a) *N*-Acetyltryptophanamide (NATA), $\lambda_{\text{ex}} = 285$ nm; $\tau = 3018$ ps, $\chi^2 = 1.17$. (b) Approximately equimolar mixture of NATA and 7-azatriptophan, $\lambda_{\text{ex}} = 285$ nm. The fluorescence decay, $I(t)$, is fit to the function $I(t) = 0.41 \exp(-t/816 \text{ ps}) + 0.59 \exp(-t/3167 \text{ ps})$, $\chi^2 = 1.16$. (c) Approximately equimolar mixture of NATA and 7-azatriptophan, $\lambda_{\text{ex}} = 305$ nm. $I(t) = 0.96 \exp(-t/817 \text{ ps}) + 0.04 \exp(-t/3906 \text{ ps})$, $\chi^2 = 1.17$. The small contribution from NATA can be further reduced by discriminating against the blue tryptophyl emission with the appropriate cutoff filter. The difference in lifetimes obtained for the long component due to NATA is a result of performing the experiment on a full scale of 6 ns where there is not enough dynamic range to fit reliably a 3-ns decay, especially in the presence of a second component. The fluorescence lifetime apparatus is similar to the one we constructed elsewhere.²⁶

mixture exhibits less than 4% contamination from tryptophyl emission (Figure 1c).

Two strategies for the use of 7-azatriptophan are immediately suggested. The first is to synthesize peptides containing one 7-azatriptophan and to study their photophysics individually. Subsequently, one can bind them to target proteins that may contain several tryptophans and study the dynamics of the model peptides in the complexes. We have synthesized the *t*-BOC derivative of 7-azatriptophan and have prepared the tripeptide NAC-Pro-7-azatrp-Asn-NH₂, which mimics the active site of the potato proteinase inhibitor II.²⁷ The fluorescence decays of both compounds are also single exponential. This behavior is unlike that of any peptide derivative of tryptophan, with the exception of the anomalous *N*-acetyltryptophanamide.^{4,7-11}

Second, Brawerman and Ycas¹⁸ and Schlesinger¹⁹ demonstrated that 7-azatriptophan can be incorporated into bacterial protein. Other methods of incorporating "nonnatural" amino acids have been developed using suppressor tRNA.^{20,21} We verified the former results^{18,19,22} with an *Escherichia coli* Trp auxotroph (ATCC 23803) containing a lysogenic λ ORF8.²³ When grown

- (5) Donzel, B.; Gauduchon, P.; Wahl, P. *J. Am. Chem. Soc.* **1974**, *96*, 801.
 (6) Gudgin, E.; Lopez-Delgado, R.; Ware, W. R. *J. Phys. Chem.* **1983**, *87*, 1559.
 (7) Chen, L. X.-Q.; Petrich, J. W.; Fleming, G. R.; Perico, A. *Chem. Phys. Lett.* **1987**, *139*, 55.
 (8) Ross, J. B. A.; Rousslang, K. W.; Brand, L. *Biochemistry* **1981**, *20*, 4361.
 (9) Werner, T. C.; Forster, L. S. *Photochem. Photobiol.* **1979**, *29*, 905.
 (10) Cockle, S. A.; Szabo, A. G. *Photochem. Photobiol.* **1981**, *34*, 23.
 (11) Szabo, A. G.; Rayner, D. M. *Biochem. Biophys. Res. Commun.* **1980**, *94*, 909.
 (12) Petrich, J. W.; Longworth, J. W.; Fleming, G. R. *Biochemistry* **1987**, *26*, 2711.
 (13) Taylor, C. A.; El-Bayoumi, M. A.; Kasha, M. *Proc. Natl. Acad. Sci. U.S.A.* **1969**, *63*, 253.
 (14) Hetherington, W. M.; Micheels, R. M.; Eisenthal, K. B. *Chem. Phys. Lett.* **1979**, *66*, 230.
 (15) Collins, S. T. *J. Phys. Chem.* **1983**, *87*, 3202.
 (16) Moog, R. S.; Bovino, S. C.; Simon, J. D. *J. Phys. Chem.* **1988**, *92*, 6545.
 (17) Ingham, K. C.; El-Bayoumi, M. A. *J. Am. Chem. Soc.* **1974**, *96*, 1674.
 (18) Brawerman, G.; Ycas, M. *Arch. Biochem. Biophys.* **1957**, *68*, 112.
 (19) Schlesinger, S. *J. Biol. Chem.* **1968**, *243*, 3877.
 (20) Noren, C. J.; Anthony-Cahill, S. J.; Griffith, M. C.; Schultz, P. G. *Science* **1989**, *244*, 182.
 (21) Bain, J. D.; Glabe, C. G.; Dix, T. A.; Chamberlin, A. R. *J. Am. Chem. Soc.* **1989**, *111*, 8013.
 (22) Pardee, A. B.; Prestidge, L. S. *Biochim. Biophys. Acta* **1958**, *27*, 330.
 (23) Meissner, P. S.; Sisk, W. P.; Berman, M. L. *Proc. Natl. Acad. Sci. U.S.A.* **1987**, *84*, 4171.
 (24) Pardee, A. B.; Jacob, F.; Monod, J. *J. Mol. Biol.* **1959**, *1*, 165.
 (25) Bradford, M. M. *Anal. Biochem.* **1976**, *72*, 248.
 (26) Chang, M. C.; Courtney, S. J.; Cross, A. J.; Gulotty, R. J.; Petrich, J. W.; Fleming, G. R. *Anal. Instrum. (N.Y.)* **1985**, *14*, 33.

- (27) Thornburg, R. W.; An, G.; Cleveland, T. E.; Ryan, C. A. *Proc. Natl. Acad. Sci. U.S.A.* **1987**, *84*, 744.

in the presence of 7-azatryptophan, this *E. coli* strain showed roughly 20% of the β -galactosidase activity of bacteria grown in tryptophan (5.3 A_{420} /mg of protein vs 28.2 A_{420} /mg of protein^{24,25}).

These data point to the importance, the versatility, and the usefulness of 7-azatryptophan as a probe of protein structure and dynamics.

Direct Measurement of Transition-State Bond Cleavage in Hydrolysis of Phosphate Esters of *p*-Nitrophenol

Alvan C. Hengge and W. W. Cleland*

Institute for Enzyme Research and the
Department of Biochemistry
University of Wisconsin, Madison, Wisconsin 53705

Received June 6, 1990

We have found a simple technique to measure the degree of bond breaking in the transition state which should be applicable to any reaction where *p*-nitrophenol is the leaving group. The breaking of a bond to *p*-nitrophenol in a displacement reaction involves the development of delocalized negative charge in the phenol corresponding to the degree of bond breaking. The delocalization of this negative charge occurs through the contribution of a quinonoid resonance form in which the bond order between nitrogen and oxygen decreases and the bond order between nitrogen and carbon increases. Since nitrogen-oxygen bonds are more stiffening than nitrogen-carbon ones, ¹⁵N will enrich in the uncharged phenol, and a normal isotope effect will be observed on formation of the phenolate anion. The size of this isotope effect in a displacement reaction affords a measure of the magnitude of charge developed on the *p*-nitrophenol leaving group in the transition state.

Though small, these isotope effects are well within the measurable range when one uses the competitive method and an isotope ratio mass spectrometer to measure isotopic discrimination. Since the spectrometer measures nitrogen as N₂, the nitrogen in the *p*-nitrophenol must be converted to N₂ via reduction, Kjeldahl digestion, and oxidation.¹ The natural abundance of ¹⁵N in the substrate serves as the label, so no synthesis of labeled substrate is necessary.²

We have determined the equilibrium ¹⁵N isotope effect for deprotonation of *p*-nitrophenol by partitioning half-ionized material between water and methylene chloride. A prior experiment with fully protonated *p*-nitrophenol determined the equilibrium constant for partitioning $K_{\text{organic/aqueous}}$ to be 6.2, and the equilibrium isotope effect on partitioning $^{15}K_{\text{part}}$ as 1.0005 ± 0.0001 .³ With half-ionized nitrophenol, all of the deprotonated compound stays in the aqueous layer and the protonated phenol partitions between the two layers. The equilibrium isotope effect on deprotonation was found to be 1.0023 ± 0.0001 .⁴

(1) The general method used in this lab for measuring ¹⁵N isotope effects has been described: Hermes, J. D.; Weiss, P. M.; Cleland, W. W. *Biochemistry* 1985, 24, 2959. A detailed description of the techniques used in the production and isolation of N₂ from nitrophenol can be found in the following: Weiss, P. M. Heavy Atom Isotope Effects Using the Isotope Ratio Mass Spectrometer. In *Enzyme Mechanisms From Isotope Effects*; Cook, P. F., Ed.; CRC Press, Inc.: Boca Raton, FL; Chapter 11, in press.

(2) Reactions are allowed to run to about 50% completion and assayed to determine the exact fraction of reaction. The product is separated from the residual substrate, the nitrogen from each separately converted to N₂, and the isotopic composition determined by the isotope ratio mass spectrometer. The isotopic composition of the starting material is separately determined. Isotope effects are calculated from the isotopic composition of the starting material and residual substrate, and independently from those of the starting material and product. The equations used for isotope effect calculations can be found in the following: O'Leary, M. H. *Methods Enzymol.* 1980, 64, 83.

(3) $^{15}K_{\text{part}}$ was calculated as $R_{\text{aqueous}}/R_{\text{organic}}$. R_{aqueous} and R_{organic} refer to the isotopic ratios of *p*-nitrophenol in the aqueous and organic layers, respectively. The isotopic ratios are the ratios of the ¹⁵N-to-¹⁴N ratio in the sample to that of a standard sample of N₂ gas, as measured by the isotope ratio mass spectrometer.

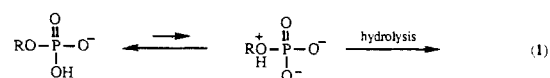
Table I. Isotope Effects on Phosphate Ester Hydrolysis Reactions and on Deprotonation of Nitrophenol

	reactn conditns ^a	¹⁴ k/ ¹⁵ k
monoester ^b	pH 4, 100 °C, 1 h	1.0004 ± 0.0002
monoester ^b	pH 10, 100 °C, 8.5 h	1.0028 ± 0.0002
diester ^c	pH 0.5, 100 °C, 14 h	1.0009 ± 0.0002
diester ^c	pH 13, 100 °C, 2.5 h	1.0016 ± 0.0002
triester ^d	pH 12, 22 °C, 15 min	1.0007 ± 0.0001
deprotonation		1.0023 ± 0.0001 ^e

^aTimes given are the half-lives for hydrolysis. ^b*p*-Nitrophenyl phosphate. ^c3,3-Dimethylbutyl *p*-nitrophenyl phosphate. ^dDiethyl *p*-nitrophenyl phosphate. ^eEquilibrium isotope effect.

The utility of this new method for probing transition-state structures is demonstrated in a study of phosphate ester hydrolysis reactions. We have measured the ¹⁵N isotope effect in the hydrolysis reactions of a phosphate monoester, a diester, and a triester with *p*-nitrophenol as the leaving group, under a variety of conditions. Our results appear in Table I.

The generally accepted mechanism^{5,6} for the hydrolysis of monoanions of phosphomonoesters involves a preequilibrium proton transfer to the bridge oxygen atom followed by P-O bond cleavage or, for good leaving groups, rate-limiting proton transfer followed by P-O bond cleavage (eq 1).



If this mechanism is correct, there will be no development of negative charge on the leaving group, and the small isotope effect may reflect the difference between an O-phosphoryl versus an O-H bond to the nitrophenol. However, MNDO, AM1, and PM3 calculations performed in our laboratory all indicate that a monoester protonated at the bridge position has no stability and therefore cannot be an intermediate. The computational and isotope effect results are consistent with a mechanism where proton transfer is driven by and lags slightly behind P-O bond fission in a concerted, asynchronous process.

The isotope effect on deprotonation might be expected to represent the upper limit for these isotope effects, since it formally represents completely breaking the bond to the phenolic oxygen. This is not the case experimentally (Table I) as the isotope effect for hydrolysis of *p*-nitrophenyl phosphate at pH 10 is larger than the deprotonation effect. There are three reasons why the equilibrium isotope effect on deprotonation will not represent the maximum observable effect. The first is the aforementioned difference between an O-P versus an O-H bond. Second, the observed equilibrium deprotonation effect in water will be diminished by hydrogen bonding of solvent to the phenolic oxygen, which will lessen the contribution of the quinonoid resonance form. In the transition state of a displacement reaction, the phenolic oxygen will not be similarly solvated. Third, and probably more important, the monoester dianion is thought⁶ to hydrolyze by a dissociative mechanism with almost no bond order to the *p*-nitrophenol leaving group. In such a transition state, the negative charge on the PO₃ unit will be in close proximity to the phenolate oxygen, and charge repulsion will increase the contribution of the quinonoid resonance form and hence the ¹⁵N isotope effect. The isotope effect observed for this reaction is thus in agreement with the accepted mechanism.

Phosphodiester undergo both acid- and base-catalyzed hydrolysis. The pH profile⁷ in the acid region indicates that the

(4) Calculated as $R_{\text{protonated}}/R_{\text{deprotonated}}$ where these values refer to the isotopic ratios of the protonated and deprotonated nitrophenol in the aqueous layer. $R_{\text{protonated}}$ was found by multiplying the isotopic ratio of nitrophenol in the organic layer by 1.0005. $R_{\text{deprotonated}}$ was calculated from $R_{\text{protonated}}$, the observed combined isotopic ratio of both species in the organic layer (R_{obsd}), and the fraction of protonated nitrophenol in the aqueous layer (f) using the equation $R_{\text{deprotonated}} = R_{\text{obsd}} - (f \times R_{\text{protonated}})/(1 - f)$.

(5) Kirby, A. J.; Varvoglis, A. G. *J. Am. Chem. Soc.* 1967, 89, 414.

(6) Benkovic, S. J.; Schray, K. J. In *Transition States of Biochemical Processes*; Gandour, R. D., Schowen, R. L., Eds.; Plenum Press: New York, 1978; Chapter 13. Westheimer, F. N. *Chem. Rev.* 1981, 81, 313.

(7) Kirby, A. J.; Younas, M. *J. Chem. Soc. B* 1970, 510.